Single-Pyranometer Approach for Diffuse Optimization in Solar Tracking Systems

João G. F. Foes[1], Rafael A. Campos[1], Lucas R. Nascimento[1], Jonas Wetzel[2], Rafael Rodrigues de Souza[2], Ricardo Rüther[1]

[1] Universidade Federal de Santa Catarina, Florianópolis (Brazil)

[2] Brametal S.A., Linhares (Brazil)

Abstract

This study presents the development and field validation of a simplified optimization algorithm for single axis tracking systems (SATS) operating under diffuse irradiance conditions. The proposed approach eliminates the need for complex meteorological stations or multiple reference cells, using instead a single pyranometer to monitor the clearness index (Kc) and control the trackers' positioning. The algorithm commands the horizontal positioning of the modules whenever Kc remains below 0.3 for more than eight minutes, returning to standard tracking (ST) once the condition is no longer met. The methodology was implemented in a 5 MWp photovoltaic plant located in southeastern Brazil, where one of the ten inverter groups was used as the optimized unit with the proposed algorithm, while the others operated under ST. Over approximately one year of continuous operation, the system achieved daily energy gains of up to 5.49% and an accumulated improvement of 0.38% in energy generation compared to the reference groups. These results demonstrate the feasibility of applying a single-sensor diffuse irradiance optimization strategy in utility-scale PV plants, offering a cost-effective and scalable alternative to current tracking control approaches.

Keywords: diffuse irradiance optimization, single-pyranometer approach, solar tracking systems, clearness index, photovoltaic performance.

1. Introduction

The growing demand for electricity in Brazil, together with the rapid expansion of the photovoltaic (PV) sector, has reinforced the need for improving the performance and efficiency of large-scale solar power plants. In 2024, solar generation in the country increased by 21% (Neves, 2025), and nearly 94% of utility-scale PV plants already operate with single-axis tracking systems (López, 2025). These trackers can deliver up to 20% higher annual energy yields compared to fixed-tilt installations under clear-sky conditions (Guarnieri, 2017). However, their performance remains suboptimal during periods dominated by diffuse irradiance, when direct sunlight is partially or totally obstructed by clouds.

Several studies have demonstrated that reorienting PV modules to a horizontal position under cloudy conditions can increase instantaneous energy generation. Kelly and Gibson (2011) and Koussa et al. (2011) observed potential daily improvements of up to 40%, although with annual gains typically limited to around 1–2%. Antonanzas et al. (2018a) also identified similar results through diffuse-irradiance optimization experiments in European climates. Despite these findings, no clear methodology or field-validated results have been reported in the literature regarding the implementation of optimization algorithms for diffuse irradiance conditions in utility-scale PV plants. Most existing studies are limited to simulation-based analyses or small experimental setups, lacking comprehensive validation under real operating environments. This gap highlights the need for a complete methodological framework supported by field results.

In this context, the present study proposes and validates a simplified optimization algorithm capable of detecting diffuse-irradiance conditions using only a single pyranometer. The algorithm employs the clearness index (K_C) as a decision parameter to command the horizontal positioning of the modules whenever K_C remains below 0.3 for more than eight minutes. The clearness index represents the ratio between the measured global horizontal irradiance (GHI) and the theoretical clear-sky GHI, serving as an indicator of atmospheric transparency — lower K_C values correspond to cloudy conditions, while higher values indicate clearer skies. This index differs from the extraterrestrial clearness index (K_T), which compares GHI with the solar irradiance outside the Earth's atmosphere. The main research gap addressed by this work lies in the complete methodological development and field validation of the proposed system under real operating conditions in a utility-scale PV plant, providing empirical evidence of its effectiveness and practical feasibility. The algorithm was implemented in collaboration with a 5 MWp PV plant located in southeastern Brazil, where it was applied to one of ten independent inverter groups while the others operated under standard

10.18086/swc.2025.03.67 Available at http://proceedings.ises.org

tracking (ST). Over approximately one year of operation, the system achieved daily energy gains of up to 5.49% and an accumulated improvement of 0.38% compared to the standard configuration, confirming the applicability of the proposed optimization strategy for industrial-scale PV plants.

2. Methodology

To implement and validate the proposed algorithm, a collaboration was established with a commercial 5 MWp PV plant located in southeastern Brazil. The plant is composed of ten independent groups, each connected to a dedicated inverter and identified by its corresponding "Skid" number. Among these, one group was selected for the implementation of the optimization algorithm, while the remaining groups continued to operate under the manufacturer's ST mode. To achieve this, a tracking operation validation was performed, intrinsic differences between inverter strings were quantified and compensated, and performance indicators were calculated to assess the energy gains achieved by the optimized strategy.

2.1. Experimental Setup

The proposed methodology aims to implement an optimization system for conditions with predominant diffuse irradiance, without requiring a complete meteorological station or reference cells mounted on the tracker, relying in a single pyranometer and open-source softwares. This simplistic approach sets a standard between white papers shared by industry manufactures (Abbaraju and Daly, 2020).

The experimental setup consisted of an RSensDB pyranometer (DualBase, Class B according to ISO 9060:2018), RJ45 communication cables, DB9 connectors, and a 12 V AC–DC power supply. Communication with the tracker control units (TCUs) was established via a Modbus gateway using IP-based protocols.

The system architecture is shown schematically in Fig. [1]. The algorithm running on the industrial PC periodically acquires and stores irradiance and operational data from all trackers in the plant. Gathering information from every tracker in the PV plant plays a crucial role, as a malfunction in a single device can affect the daily energy generation of the entire PV string and potentially invalidate a day of analysis. After executing the control logic described in Section 2.6, the industrial PC communicates the updated tracking position to the TCU of the selected group (Skid 3 – Inverter 1).

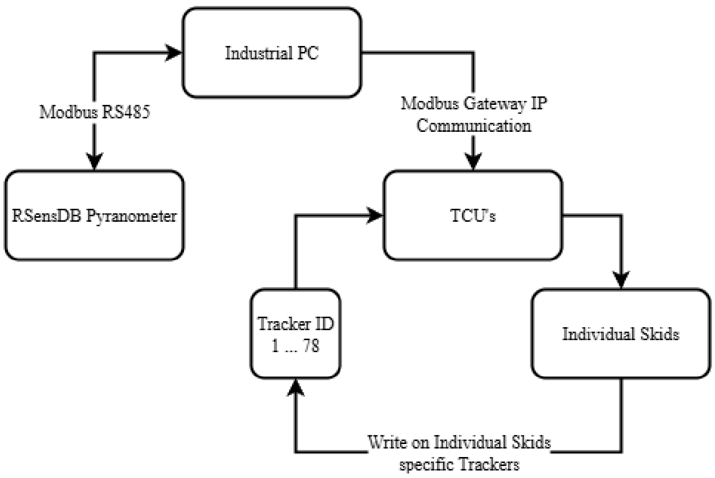

Figure 1: Flux gram representing the Communication of the Experiment.

2.2. Clearness Index (K_C) Threshold

The efficiency of the proposed algorithm is directly linked to the threshold that determines when the trackers should move to the horizontal position. Since the chosen performance metric is the clearness index (K_C), due to its simplicity of implementation, it is necessary to define the threshold value that triggers this positioning change. To establish this threshold, simulations were carried out using the PVsyst software with annual irradiance data from the *Brazilian Solar Energy Atlas* (Martins et al., 2017). Global Horizontal Irradiance (GHI) and Global Plane of Array Irradiance (GPOA) values were compared to assess the relative performance under different sky conditions. As seen in Fig. [2], it is possible to visualize that for K_C values below 0.3, the irradiance predominance is related to the GHI. This allows the conclusion that if this threshold is met, energy benefits will occur from moving the trackers horizontally.

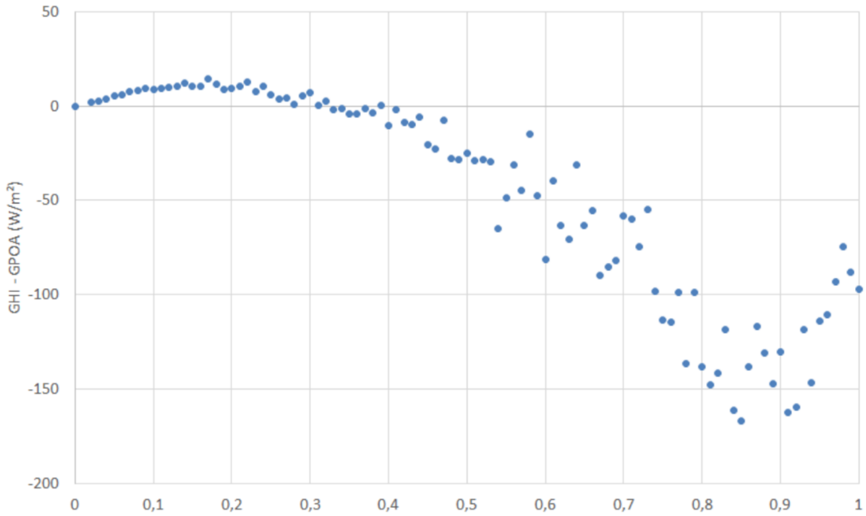

Figure 2: GHI versus GPOA for Different K_C Values.

2.3. Persistence Criterion

The persistence value defines the time window during which the K_C, established in Section 2.2, must remain below the threshold before triggering the horizontal positioning of the trackers. The establishment of a reliable persistence value ensures that the tracker won't get activated in periods where the K_C threshold is just momentarily surpassed.

The chart in Fig. [3] illustrates the measured GHI in the orange line and the red dotted line represents the K_C threshold throughout the day. It is easy to visualize that GHI surpasses K_C a few times during the day, but it never keeps its value consistently below the threshold. If activations to horizontal positioning were made in these moments, the tracker wouldn't have enough time to reach its horizontal positioning and would need to return for ST movement. This implies wasted electrical energy that wouldn't result in energy generation benefits, since the optimal positioning would never be reached.

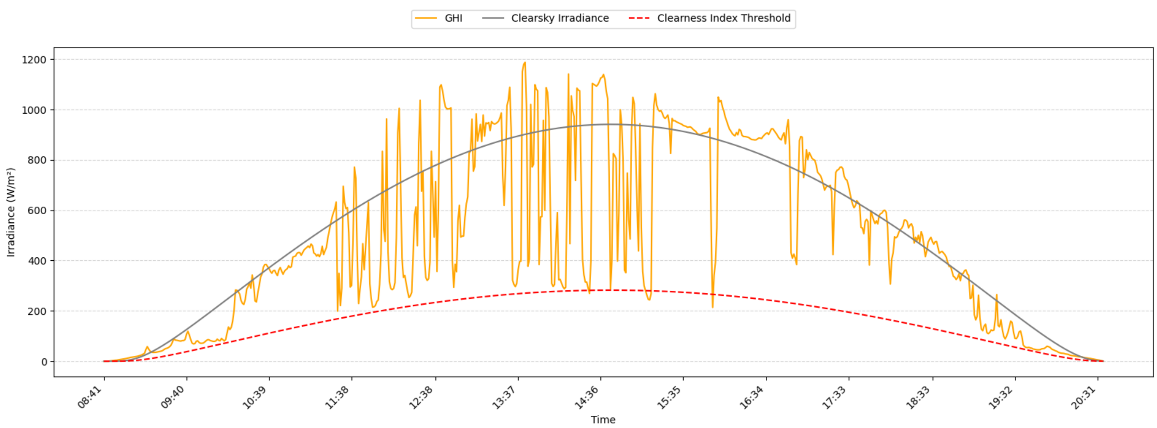

Figure 3: GHI and Clearness Index Threshold.

To avoid scenarios like the one illustrated above, a persistence threshold must be implied. A study implementing optimized diffused under simulated circumstances across Europe (Antonanzas et al., 2018b) applied the condition for its persistence threshold definition relating to the angular velocity of the trackers. Under the same criteria, the definition of persistence threshold was established according to the angular velocity of 0.02 RPM of the used trackers in the Solar PV Plant. This concludes that, for the worst-case scenario it would take eight minutes and 20 seconds to move to the horizontal position, hence, a persistence value of eight minutes was applied in the algorithm.

2.4. Intrinsic Inverter Difference Analysis

In large-scale PV plants composed of hundreds of modules connected to multiple inverters, intrinsic differences between the strings must be accounted to evaluate properly the energy yield by each string. Those differences may arise from module power tolerance mismatches, thermal gradients leading to localized temperature-induced power losses, or non-uniform soiling across the array (Jathar et al., 2023).

Several approaches were evaluated to represent this intrinsic difference, including: (i) calculating the mean difference over the entire period; (ii) computing average differences as a function of clearness index ranges; and (iii) applying a linear regression model to represent how these differences vary with the clearness index. The final adopted methodology used a linear regression model, implemented with the Python *scikit-learn* library, to describe the relationship between inverter energy differences and clearness index values. The resulting regression function, computed for each inverter pair, was then applied to correct the generation data during the optimization period according to the clearness index of each day.

The final evaluation considered a total of 92 selected dates starting from November 29 where ST was held throughout the full day of analysis in all PV plant groups.

2.5. Performance Evaluation

The assessment of the algorithm's performance was based on the comparison between the energy generated by the optimized group and that of the reference groups. For each reference inverter, the energy difference (in MWh) was calculated as the energy produced by the optimized group, corrected by its intrinsic difference, minus the energy generated by the corresponding reference group.

From this comparison, three key indicators were obtained: the absolute energy difference (MWh), the percentage energy difference (%), and the cumulative percentual difference in energy generation (%) over the analyzed period.

These indicators enabled an individual performance evaluation for each group, highlighting the days with the highest relative gains in efficiency.

2.6. Algorithm Logic

To illustrate the workflow of the implemented algorithm, Fig. [4] illustrates the logical workflow of the implemented algorithm. The system continuously acquires irradiance data from the pyranometer for an eight-minute period, with a temporal resolution of ten seconds. At the end of each minute, the average irradiance value is computed to minimize potential discrepancies caused by transient cloud passages. If the K_C defined in Section 2.3 is maintained throughout the entire persistence period, the algorithm commands the horizontal positioning of the selected group; otherwise, the ST mode remains active.

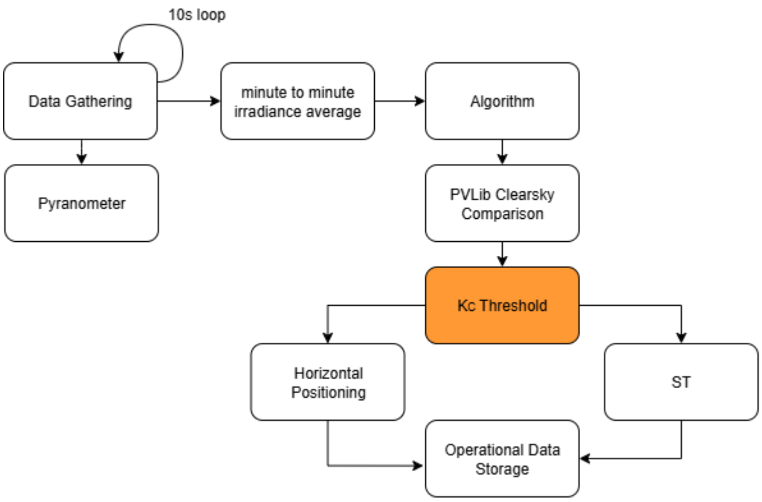

Figure 4: Fluxogram of Proposed Algorithm Workflow.

3. Results and Discussions

To evaluate the results obtained throughout the study, data were collected between November 29th and October 13th, covering roughly one year of system operation. During this period, analysis concentrated on comparing performance between the optimized tracking algorithm and the ST configuration. The primary evaluation metric was the accumulated percentage difference, obtained from daily percentage variations in energy generation between both tracking approaches. This indicator provides a broader view of long-term system behavior, minimizing daily fluctuations and emphasizing consistent trends in energy gain.

3.1. Persistence Threshold Evaluation

To verify that applying an eight minute persistence for the clearness index threshold is consistent with the continuous presence of cloudy conditions, the duration of each horizontal positioning event was analyzed. Fig. [4] presents a histogram illustrating the most frequent durations during which the tracker remains in the horizontal position after being activated.

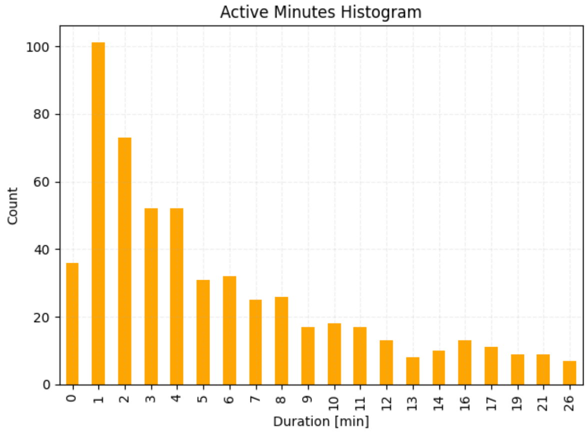

Figure 4: Histogram of most minutes in horizontal positioning after activation.

The analysis revealed that, on average, the tracker remains in the horizontal position for approximately 52 minutes after each activation. This finding is significant, as it indicates that once the horizontal positioning is triggered, the atmospheric condition under which the system operates more efficiently in the horizontal state tends to persist for an extended period. Consequently, the eight minute persistence criterion adopted for the clearness index threshold proves to be an appropriate and robust parameter for identifying genuinely cloudy conditions.

3.2. Energy Gain Analysis

The first result concerns the accumulated energy generated during the evaluation period. Fig. [5] presents the daily energy yield for both configurations — the optimized tracking system and the ST mode — along with the accumulated percentage difference and the daily percentage variation between them. In the bar chart, the dark gray bars represent the daily energy generated by the optimized group, while the light gray bars correspond to the ST group. The green line indicates the daily percentage gain, and the orange line shows the accumulated percentage difference throughout the analyzed period. The results indicate daily percentage peaks of approximately 6% in favor of the optimized system, while the total accumulated difference over the analyzed period reached 0.38%.

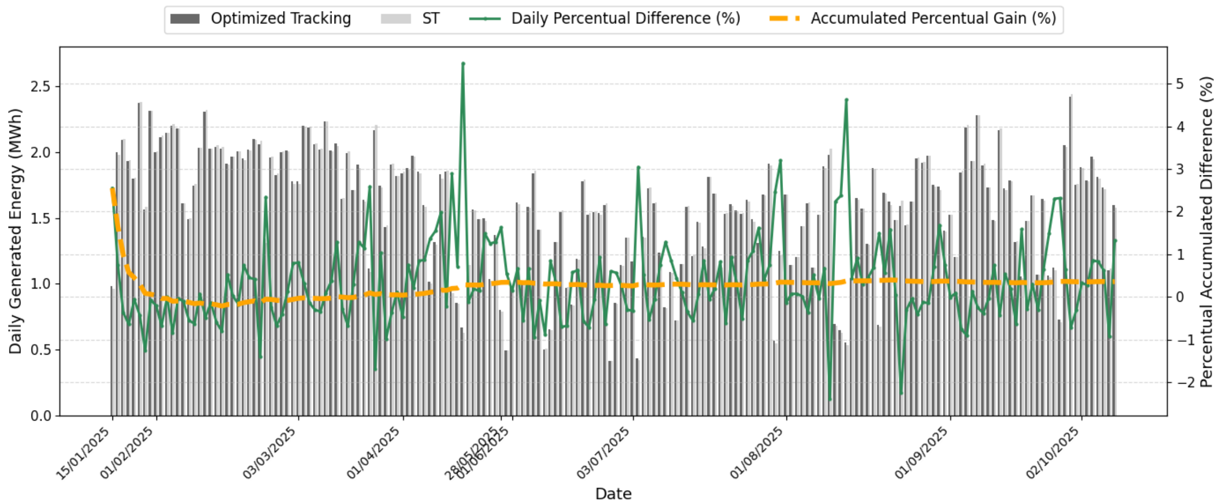

Figure 5: Daily Energy and Percentual Difference Analysis.

Table [1] presents the ten days with the highest energy gains recorded during the evaluation period, including the energy generated by both configurations, the corresponding K_C, and the percentage difference. The results allow an analysis showing that, although the long-term energy benefit is close to 0.4%, much higher gains can be observed on individual days characterized by predominantly cloudy conditions, with daily energy increases reaching up to 5.49%.

Table 1: 10 Days with Highest Energy Gains during the Evaluation Period.

Date	Optimized Group Generated Energy (MWh)	ST Group Generated Energy (MWh)	K_C	Percentual Gain (%)
18/04	0,67	0,63	0.25	5,49
12/08	0,55	0,53	0.22	4.62
31/07	1,25	1,21	0,59	3,20
04/07	0,43	0,42	0,20	3,05
18/03	0,96	0,93	0,39	2,89
15/01	1,12	1,09	0,43	2,59
30/07	0,98	0,96	0,35	2,55
11/08	0,56	0,55	0,24	2,46
22/02	0,64	0,63	0,27	2,38
25/09	0,73	0,71	0,25	2,32

To illustrate the irradiance behavior on the day with the highest energy gains, Fig. [6] shows the GHI profile for April 18th, 2025, when the system achieved a 5.49% energy benefit. For comparison, Fig. [7] presents data from September 25th, 2025, a day with lower performance. The contrast between these two cases indicates that activations occurring during periods of peak clearsky irradiance contribute more significantly to overall energy gains than those taking place near sunrise or sunset. This suggests that future analyses with higher temporal resolution could provide deeper insights into the specific moments of the day when horizontal positioning yields the greatest benefit.

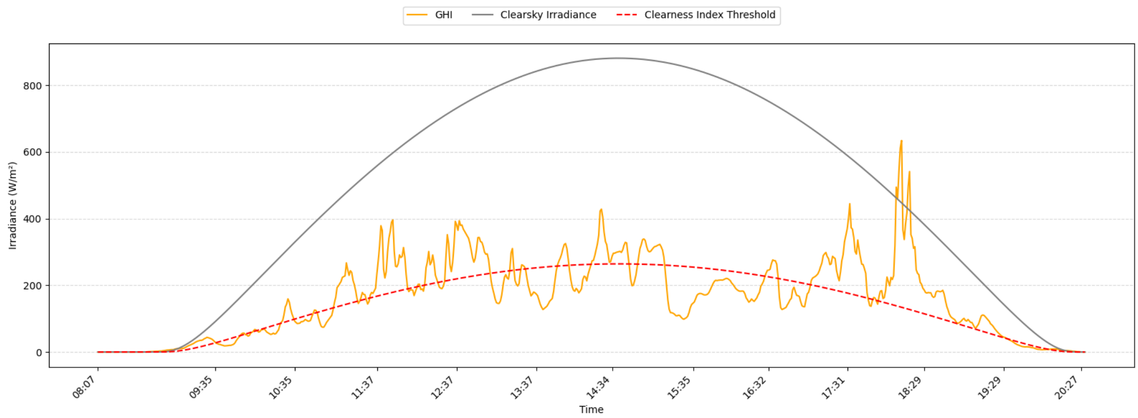

Figure 6: GHI and K_C Threshold for 2025-04-18.

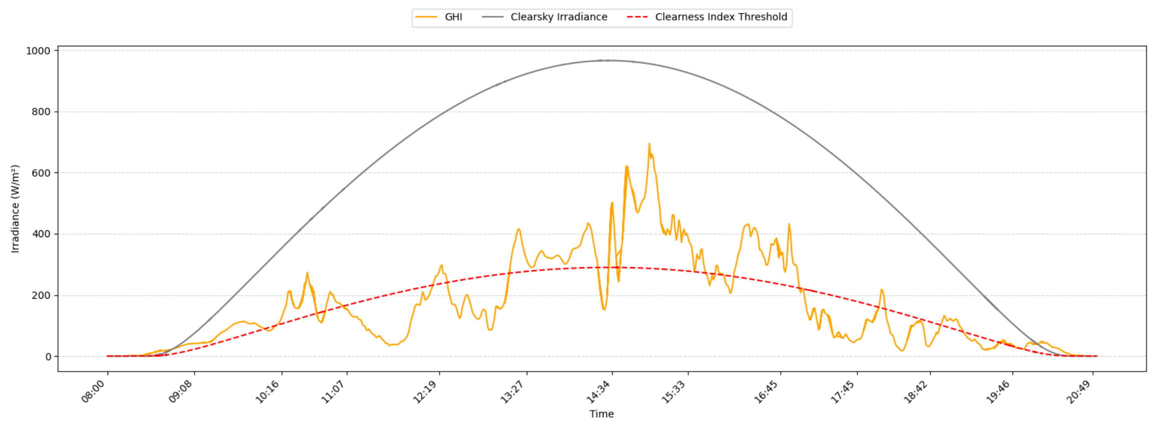

Figure 7: GHI and K_C Threshold for 2025-04-18.

The chart presented in Fig. [8] illustrates the relationship between the K_C and the percentage difference in daily energy generation. Each point represents a day of operation, colored according to the number of active minutes of the algorithm. A negative correlation between Kc and the percentage difference can be observed, indicating that **the algorithm tends to provide higher energy gains on days with lower clearness index values**, typically associated with cloudier conditions. It is also noticeable that several days show a high number of activations even when the average Kc is above 0.3, corresponding to days with short but intense periods of cloud cover.

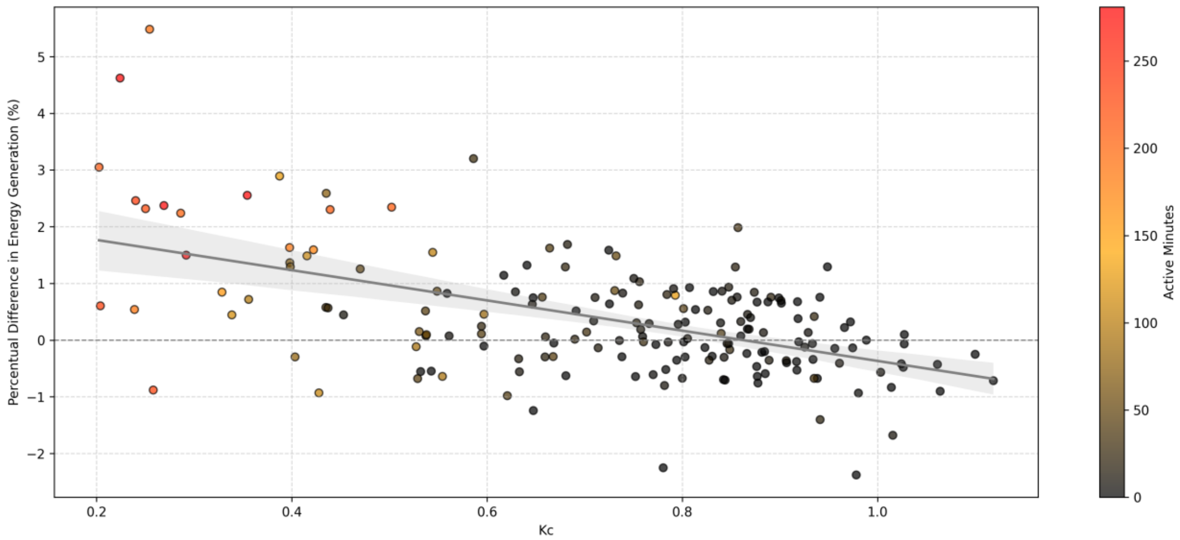

Figure 8: Daily Percentual Energy Difference *versus* Clearness Index.

Some additional factors may influence the interpretation of the presented results. While aggregating energy data on a daily timescale limits the temporal resolution of the algorithm's behavior and its effects throughout the day, it also enhances the spatial representativeness of irradiance conditions across the entire PV plant. It should also be noted that the algorithm's performance may have been constrained by the persistence criterion being applied only to trigger the horizontal positioning of the modules, and not to their return to ST operation. Further studies could address this limitation to assess its potential impact on overall performance.

Since the analyzed system is composed of monofacial modules, the present study did not account for possible consequences of the algorithm's operation in cases where albedo irradiance significantly contributes to energy generation. Considering the increasing adoption of bifacial technology in utility-scale PV plants, future work should include an analysis of the algorithm's behavior under conditions influenced by ground-reflected irradiance.

Finally, regional seasonality and economic aspects must also be considered when assessing the relevance of the proposed approach. Optimization of diffuse irradiance utilization is expected to be less significant in regions with lower cloud coverage compared to those characterized by prolonged cloudy periods. As a reference, the average KC observed during the analyzed period at the PV plant was 0.72. Even though the cost of PV modules has decreased in recent years, expanding plant capacity still requires higher implementation costs and infrastructure adjustments. In contrast, the integration of intelligent or optimized tracking algorithms represents a simple and low-cost strategy to enhance energy generation without major structural modifications.

4. Conclusions

The results obtained from nearly one year of field operation confirm that the proposed single-pyranometer methodology for optimizing diffuse irradiance under cloudy conditions provides measurable energy benefits and effectively adapts its tracking behavior according to real-time irradiance conditions. By applying a clearness index threshold of 0.3 and a persistence criterion of eight minutes, the system achieved a cumulative energy gain of 0.38% over the evaluation period, with daily gains reaching up to 5.49% during predominantly cloudy days. Additionally, a dispersion analysis illustrates the relationship between the algorithm's percentage gain and different clearness index values, confirming its intended behavior of enhancing energy generation during diffuse irradiance conditions.

The proposed approach demonstrates an economically viable, simple, and scalable solution for utility-scale PV plants, offering a complete methodology supported by field-validated results. Future work should include evaluations with bifacial modules to assess trade-offs related to albedo irradiance and horizontal positioning, the implementation of a persistence definition for returning to ST, spatial representativeness studies of single-pyranometer measurements for scalability assessment, and analyses of I–V curves to determine specific times of the day when horizontal positioning provides greater benefits.

5. Acknowledgments

This research was carried out within the scope of the activities of the National Institute for Technological Development of Photovoltaic Solar Energy Applications, INCT-DAESF, CNPq/MCTI/Brazil, Grant No. 408486/2024-4.

References

Abbaraju, V., Daly, A., 2020. Optimizing your energy yield. NEXTracker, Whitepaper.

Antonanzas, J., Urraca, R., Martinez-de-Pison, F.J., Antonanzas, F., 2018a. Optimal solar tracking strategy to increase irradiance in the plane of array under cloudy conditions: A study across Europe. Solar Energy 163, 122–130. https://doi.org/10.1016/j.solener.2018.01.080

Antonanzas, J., Urraca, R., Martinez-de-Pison, F.J., Antonanzas, F., 2018b. Optimal solar tracking strategy to increase irradiance in the plane of array under cloudy conditions: A study across Europe. Solar Energy 163, 122–130. https://doi.org/10.1016/j.solener.2018.01.080

Guarnieri, M.V., 2017. Usinas solares fotovoltaicas com seguimento em um eixo no Brasil: aspectos da construção, custos e expectativa de desempenho. Master Thesis. Universidade Federal de Santa Catarina - UFSC.

Jathar, L.D., Ganesan, S., Awasarmol, U., Nikam, K., Shahapurkar, K., Soudagar, M.E.M., Fayaz, H., El-Shafay, A.S., Kalam, M.A., Bouadila, S., Baddadi, S., Tirth, V., Nizami, A.S., Lam, S.S., Rehan, M., 2023. Comprehensive review of environmental factors influencing the performance of photovoltaic panels: Concern over emissions at various phases throughout the lifecycle. Environmental Pollution 326, 121474. https://doi.org/10.1016/J.ENVPOL.2023.121474

Kelly, N.A., Gibson, T.L., 2011. Increasing the solar photovoltaic energy capture on sunny and cloudy days. Solar Energy 85, 111–125. https://doi.org/10.1016/j.solener.2010.10.015

Koussa, M., Cheknane, A., Hadji, S., Haddadi, M., Noureddine, S., 2011. Measured and modelled improvement in solar energy yield from flat plate photovoltaic systems utilizing different tracking systems and under a range of environmental conditions. Appl Energy 88, 1756–1771. https://doi.org/10.1016/j.apenergy.2010.12.002

López, D., 2025. Brazil: renewable energy and system preferences from Trends Report 2025 [WWW Document]. RatedPower. URL https://ratedpower.com/blog/brazil-renewable-energy-trends/ (accessed 6.23.25).

Martins, F.R., Pereira, E.B., Gonçalves, A.R., Costa, R.S., Lima, F.J., Rüther, R., Abreu, S. de L., Tiepolo, G.M., Pereira, S.V., Souza, J.G. de, 2017. Atlas brasileiro de energia solar.

Neves, L., 2025. Brazil to add 19.2 GW of solar capacity in 2025 [WWW Document]. PV Magazine. URL https://www.pv-magazine.com/2025/05/09/brazil-to-add-19-2-gw-of-solar-capacity-in-2025/ (accessed 6.23.25).